Renal elasticity and perfusion changes on ultrasonography in an early-stage diabetic rat model

Yan Li[1,2], Zi-Shuo Liu[2], Ran Wei[3,4], Zhi-Wen Liu[2], Li-Xin Guo[3,4], Jun-Hong Ren[1,2]

[1]Department of Sonography, Graduate School of Peking Union Medical College, Beijing, China; [2]Department of Sonography, Beijing Hospital, National Center of Gerontology, Institute of Geriatric Medicine, Chinese Academy of Medical Sciences, Beijing, China; [3]Department of Endocrinology, Peking University Fifth School of Clinical Medicine, Beijing, China; [4]Department of Endocrinology, Beijing Hospital, National Center of Gerontology, Institute of Geriatric Medicine, Chinese Academy of Medical Sciences, Beijing, China

Contributions: (I) Conception and design: JH Ren, LX Guo; (II) Administrative support: JH Ren, ZW Liu; (III) Provision of study materials or patients: R Wei; (IV) Collection and assembly of data: ZS Liu, Y Li; (V) Data analysis and interpretation: Y Li, R Wei; (VI) Manuscript writing: All authors; (VII) Final approval of manuscript: All authors.

Correspondence to: Jun-Hong Ren, MM. Department of Sonography, Graduate School of Peking Union Medical College, Beijing 100005, China; Department of Sonography, Beijing Hospital, National Center of Gerontology, Institute of Geriatric Medicine, Chinese Academy of Medical Sciences, No. 1 Dahua Road, Dongcheng District, Beijing 100730, China. Email: rjh13910813603@163.com.

Background: Renal hemodynamic changes in early diabetes occur before the onset of significant structural abnormalities or clinical manifestations, and timely detection of these changes has clinical significance. This study aimed to evaluate renal elasticity and perfusion changes in an early-stage diabetic rat model by shear wave elastography (SWE) and contrast-enhanced ultrasound (CEUS), and to explore the potential correlations between renal elasticity and perfusion parameters.

Methods: A total of 18 male Sprague-Dawley rats were randomly divided into three groups: a control group (group 1, n=6), a diabetic group (group 2, n=6), and a diabetic group receiving drug therapy (group 3, n=6). An intraperitoneal injection of streptozotocin (STZ) for 2 days combined with a high-fat diet (HFD) was used as the early-stage diabetic rat model. The diabetic rats in group 3 were treated with canagliflozin and losartan for 6 weeks, whereas the rats in groups 1 and 2 were given equal amounts of purified water. Renal stiffness on SWE and perfusion parameters on CEUS were measured and compared among the three groups, then the rats were sacrificed, and serum, urine, and renal histopathology were evaluated to confirm the development of early diabetes.

Results: The early-stage diabetic rats without significant pathological changes exhibited bigger kidneys and higher blood glucose (all P<0.05). Among the CEUS parameters, peak enhancement (PE), wash-in area under the curve (WiAUC), wash-in perfusion index (WiPI), wash-out AUC (WoAUC), wash-in and wash-out AUC (WiWoAUC), rise time (RT), and time to peak (TTP) of diabetic rats in group 2 were significantly increased (all P<0.05), and the hyperperfusion ameliorated significantly after drug treatment. The renal elasticity measured by SWE varied in accordance with certain perfusion parameters, and was strongly positively correlated with WiAUC (r=0.701, P<0.001), WoAUC (r=0.647, P<0.001), and WiWoAUC (r=0.655, P<0.001), and moderately positively correlated with PE (r=0.539, P=0.001), WiPI (r=0.555, P<0.001), RT (r=0.425, P=0.010), and TTP (r=0.439, P=0.007).

Conclusions: Renal elasticity and perfusion changes in the early stage of diabetes, and renal elasticity was positively associated with delayed and increased perfusion.

Keywords: Contrast-enhanced ultrasound (CEUS); shear wave elastography (SWE); diabetes; renal perfusion

Introduction

Diabetic kidney disease (DKD) is reported to occur in 20–50% of individuals with diabetes mellitus (DM), and can lead to end-stage kidney disease and increase cardiovascular morbidity and mortality (1). DKD is traditionally characterized by the development of albuminuria and a subsequent decline in the glomerular filtration rate (GFR) (2). However, when these manifestations occur, the kidneys often have irreversible pathological changes such as glomerular sclerosis. Increasing evidence indicates that renal hemodynamic changes induced by hyperglycemia are the primary factors in the occurrence and progression of renal insufficiency in early diabetes (3), so early detection of renal perfusion changes holds clinical significance.

Several methods are currently in clinical use for assessment of kidney perfusion and each technique has its own advantages and drawbacks. The clearance of para-amino-hippurate (PAH) is one of the gold standards to assess renal blood flow, but it is cumbersome, time-consuming, and underused in clinical practice. Radionuclide imaging plays a crucial role in assessing renal perfusion and can provide more information on split and total renal function (4). However, its application is limited due to radiation exposure. Dynamic contrast-enhanced computed tomography (DCE-CT) is also a reliable tool for measuring single-kidney perfusion (5), but some patients may experience the complication of contrast-induced nephropathy (6). Dynamic contrast-enhanced magnetic resonance imaging (DCE-MRI) and non-contrast-enhanced methods, such as arterial spin labeling (ASL) and intravoxel incoherent motion (IVIM), have been proposed as alternatives to radioisotope techniques and DCE-CT to evaluate renal perfusion due to the lack of radiation (7). However, susceptibility to motion and low signal-to-noise ratio (SNR) may limit their clinical application (8). Thus, it is essential to develop more safe and convenient tools to detect renal perfusion abnormalities in the early stage of diabetes. Contrast-enhanced ultrasound (CEUS) is considered a promising technique for evaluating renal microvascular perfusion and providing a more comprehensive assessment of kidney diseases (9). The contrast agents used in CEUS are strictly intravascular,

consisting mainly of tiny gas-filled microbubbles of similar size to red blood cells. The microbubble-based contrast agents can be regarded as red blood cell tracers and principally metabolized by lung exhalation, so the amount of contrast media can reflect blood flow without risk of nephrotoxicity (10). Through specialized analysis software, the signal intensity of the region of interest (ROI) can be quantified, and a mathematical fitting curve describing the time-intensity and related perfusion parameters can be obtained. Recently, the evaluation of renal blood flow with CEUS to assess the severity of acute kidney injury (AKI) or chronic kidney disease (CKD) has shown promising results in both animals and humans (11-13). However, few studies have focused on renal perfusion in early DM before irreversible pathological changes occur in the kidney.

Ultrasound elastography is a noninvasive technique to measure tissue stiffness of which shear wave elastography (SWE) is one of the commonly used methods. The ultrasonic probe emits an acoustic radiation force impulse (ARFI) to generate shear waves which extend laterally in tissue and can be measured by an ultrasonic instrument (14). The speed of shear waves can be used to calculate tissue stiffness because they propagate faster in harder tissue than they do in softer tissue. It has been shown that tissue stiffness measured by SWE positively correlates with certain pathological conditions, including breast cancer (15) and liver fibrosis (16). Recently, this method has also been utilized to assess kidney disease, including in kidney transplant patients. The majority of prior studies have indicated a positive correlation between tissue stiffness and the presence of fibrosis in the kidneys (17-19), However, other studies have reported no significant correlation between SWE measurements and pathological indicators of fibrosis in the kidneys, and abnormal tissue perfusion has been proposed as a potential factor contributing to the mismatch (20,21).

Therefore, the purpose of this study was to evaluate renal elasticity and perfusion changes before and after treatment in an early-stage diabetic rat model by noninvasive SWE and CEUS, and to identify the potential relationship between renal elasticity and perfusion parameters to provide basis for early detection and timely treatment. We present this article in accordance with the ARRIVE reporting

checklist (available at https://qims.amegroups.com/article/view/10.21037/qims-23-409/rc).

Methods

Animals and model establishment

The study was approved by the Biomedical Ethics Committee of Peking University (No. LA2021585), in compliance with international Association for Assessment and Accreditation of Laboratory Animal Care (AAALAC) guidelines for the care and use of animals. This study involved 18 male Sprague-Dawley rats (6 weeks old, 130–180 g) purchased from Huafukang (Beijing, China). In a specific-pathogen-free barrier environment, all rats were kept in a temperature-controlled environment (22–23 ℃) with a 12-hour light/dark cycle. All rats were randomly grouped using the standard = RAND() function in Microsoft Excel after 2 weeks of acclimation. Then, six rats were randomly selected as the control group (group 1) and fed standard rat chow, and 12 rats were selected as the diabetic group and fed with high-glucose and high-fat diet (HFD), containing 10% lard oil, 20% sucrose, 0.5% sodium cholate, and 2.5% cholesterol for 2 weeks. The diabetic rat model was developed after 16–24 hours of food restriction, followed by an intraperitoneal injection of streptozotocin (STZ, 40 mg/kg body weight) dissolved in ice-cold sodium citrate buffer (0.1 M, pH 4.4) for 2 consecutive days, and rats in group 1 were injected with comparable volume of sodium citrate buffer. At 3 days after STZ injection, rats with tail fasting blood glucose (FBG) >16.7 mmol/L measured using a glucometer (WEGO, Weihai, China) were considered diabetic rats (22).

Next, the 12 diabetic rats were divided into two groups randomly, one group (group 3) underwent gavage with canagliflozin (10 mg/kg/d) and losartan (30 mg/kg/d), and the other group (group 2) underwent gavage with purified water once a day. In addition, the six rats in the control group were also gavaged with equal amounts of purified water every day. After 6 weeks of treatment, all rats were sacrificed, at 16–17 weeks of age, under isoflurane anesthesia.

Measurements of blood pressure

The mean arterial pressure (MAP) of each rat was measured with a rat intelligent non-invasive blood pressure meter (model: BP-2010A; Softron Biotechnology Co., Ltd., Beijing, China).

Quantification of renal stiffness by SWE

Each rat was anesthetized by an intraperitoneal injection of 3.5 mL/kg 10% chloral hydrate solution after weighing. Bilateral flank skin was prepared by shaving and the rat was placed on the console in a supine position. The instrument used in this study was an Aplio i800 system (Canon Medical Systems Corp., Otawara, Japan) equipped with a PLI-1205BX transducer and a PLT-704SBT transducer. SWE was performed before CEUS with the PLI-1205BX transducer with a frequency of 5–18 MHz. For SWE, a maximum display setting of 120 kPa was used, and color mapping representing stiffness with the color red indicating hard elasticity and the color blue indicating soft elasticity. Stiffness, recorded as Young's modulus in units of kilopascals, was measured in the mid-portion of the renal cortex of each rat at least five times in the longitudinal plane, and the mean value was calculated (*Figure 1*).

CEUS examination

CEUS examinations were performed using the PLT-704SBT probe with a frequency of 4–11 MHz. The long axis of the kidney was displayed under B-mode imaging, and then converted into the CEUS mode with machine parameters as follows: depth 3.0 cm, mechanical index (MI) 0.10, frame rate 10 fps, gain 65 dB, dynamic range (DR) 60 dB, and focus below the kidney. We used sulfur hexafluoride microbubble contrast agent (SonoVue, Bracco, Italy) dissolved in 5 mL sterile 0.9% saline and a total of 0.4 mL/kg of contrast agent was bolus injected through the tail vein, followed by a 0.5 mL flush of 0.9% saline. Perfusion images were stored continuously for 3 minutes starting with the beginning of the flush. These procedures were repeated for each kidney in each rat and the time interval between two CEUS examinations was more than 10 minutes.

CEUS image analysis

All CEUS images were exported in the Digital Imaging and Communications in Medicine (DICOM) format and analyzed with VueBox 7.0 software (Bracco Suisse SA, Cadempino, Switzerland) dedicated for CEUS quantitative analysis. The circular ROI with a 0.03 cm^2 area was placed in the middle pole of the renal cortex (*Figure 2*) and motion compensation was launched, then the software automatically
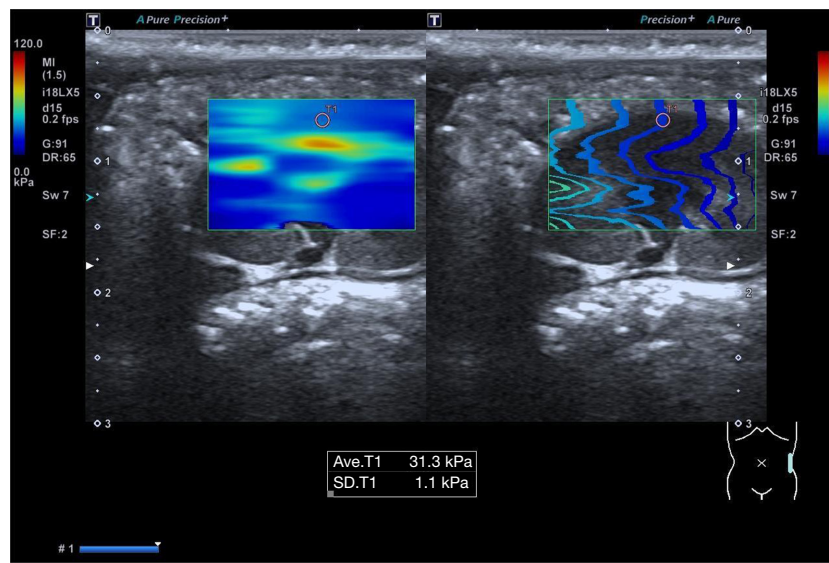
Figure 1 Measurement of elasticity in the mid-portion of the renal cortex in the longitudinal plane. Ave and SD values describe the elasticity of the measured tissue. The color map is the distribution of elasticity values scaled from 0 to 120 kPa. Ave, average; SD, standard deviation.
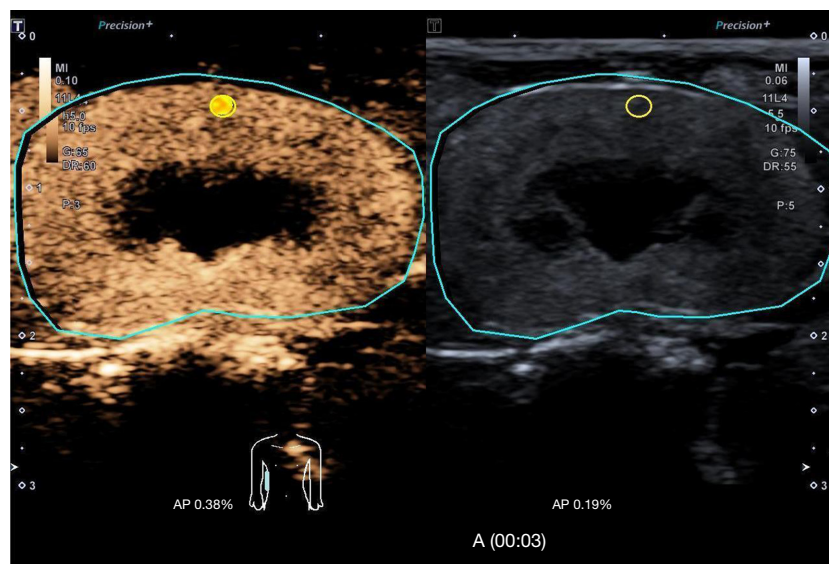

Figure 2 The ROI was placed in the middle pole of the renal cortex in CEUS quantitative analysis. AP, acoustic power, A, time A; ROI, region of interest; CEUS, contrast-enhanced ultrasound.

generated a time-intensity curve (TIC) and numerous amplitude and time parameters reflecting both blood flow and blood volume were obtained using a curve-fitting approach with a parametric perfusion model, as shown in *Figure 3*. To guarantee the quality and objectivity of the data analysis, all videos were blind processed by an experienced sonographer, and the fitting quality was greater than 75%.

Serum biochemical analysis

Blood samples were collected from the tail vein of each rat after fasting for 12 hours for the measurement of blood
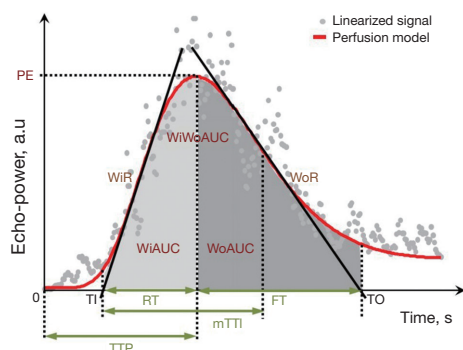
Figure 3 CEUS perfusion model and quantitative parameters. The linearized signal represents echo-power data as a function of time. TI is the instant at which the maximum slope tangent (WiR) intersects the X-axis, and TO is the instant at which the minimum slope tangent intersects the X-axis. Figure source: Bracco—VueBox® User Manual—Bracco Suisse SA; Copyright © 2010 Bracco Suisse SA all rights reserved. a.u, arbitrary unit; PE, peak enhancement; WiWoAUC, wash-in and wash-out area under the curve (WiAUC + WoAUC); WiR, wash-in rate (maximum slope); WoR, wash-out rate (minimum slope); WiAUC, wash-in area under the curve {AUC [TI:TTP]}; AUC, area under the curve; WoAUC, wash-out area under the curve {AUC [TTP:TO]}; RT, rise time (TTP – TI); FT, fall time (TO – TTP); mTTl, mean transit time local (mTT – TI); mTT, mean transit time; TTP, time to peak; CEUS, contrast-enhanced ultrasound.

using a glucose meter (WEGO). At the end of experiments, blood samples were rapidly collected at the time of euthanasia by cardiac puncture. Whole blood samples of rats should be placed at room temperature for 2 hours or overnight at 4 ℃, and then separated from the heart at 2–8 ℃ at 3,000 rpm for 15 minutes. Blood samples were used for biochemical assays of blood urea nitrogen (BUN) and serum creatinine (Scr) (Servicebio, Wuhan, China).

Urine analysis

At 16 weeks, the 18 rats were individually housed in metabolic cages with free access to water for collection of 24-hour urine specimens. According to the manufacturer's instructions (Nanjing Jiancheng Bioengineering Institute, Nanjing, China), the amount of urinary protein excreted was determined by the urine protein test kit (Coomassie brilliant blue method). The activity of urine N-acetyl-glucosaminidase (NAG) was determined by the β-NAG assay kit (colorimetric method). The amount of urine creatinine (Ucr) was determined by the creatinine assay kit

(sarcosine oxidase).

Measurement of kidney weight and calculation of kidney index

To measure kidney weight, the bilateral kidneys of each rat were removed and decapsulated. The decapsulated kidneys were placed in tissue paper for 1 minute, then transferred to a scale and weighed. The renal index (mg/g) was calculated as follows: renal index = kidney weight (mg)/body weight (g).

Tissue collection and histopathological examination

Renal tissues of each rat were fixed in 4% paraformaldehyde solution, embedded in paraffin, and cut at 3 μm thickness. Sections of kidneys in each group were stained with hematoxylin and eosin (H&E) and periodic acid-Schiff (PAS) for general morphological analysis, and Masson for renal fibrosis assessment according to the manufacturer's instructions.

Statistical analysis

Data were expressed as mean ± standard deviation (SD) or median and 25–75% interquartile range (IQR). Data that were normally distributed were analyzed with a one-way analysis of variance (ANOVA). Otherwise, the non-parametric Kruskal-Wallis H test was used, with Bonferroni correction for multiple comparisons. Pearson correlation coefficient or Spearman rank correlation coefficient was used to determine correlation between the tissue stiffness by SWE and CEUS parameters.

Statistical analyses were performed with SPSS version 26.0 software (IBM Corp., Armonk, NY, USA) and Prism 8.0 (GraphPad Software, San Diego, CA, USA). All P values were two-sided and P<0.05 was considered statistically significant.

Results

No adverse events were observed during the course of the study. General features and serum and urine biochemical parameters are displayed in *Table 1*. Compared with the control group (group 1), the kidney weight and blood glucose of diabetic rats (group 2) were significantly increased, and the difference was statistically significant (P<0.05). After 6 weeks of daily treatment with canagliflozin (10 mg/kg/d) and losartan (30 mg/kg/d), the kidney weight

Table 1 General features of experimental animals

Features	Group 1, n=6	Group 2, n=6	Group 3, n=6	P value
Body weight (g)	312.10 (25.03)	328.13 (35.00)	365.54 (34.13)	0.058
Kidney weight (mg)	1,650 (230)	2,240 (170)	1,890 (190)	0.014
Kidney weight/body weight (mg/g)	5.38 (0.94)	6.91 (1.14)	5.14 (0.90)	0.097
Blood glucose (mmol/L)	7.14 (0.81)	21.88 (2.75)	11.28 (2.71)	<0.001
BUN (mg/dL)	19.98 (1.87)	22.06 (4.96)	20.90 (4.55)	0.320
Scr (µmol/L)	58.91 (8.68)	43.54 (10.57)	64.45 (8.18)	0.549
Ucr (µmol/L)	508.70 (49.12)	1,048.15 (87.61)	578.43 (53.92)	0.011
Urine NAG activity (U/L)	29.68 (14.33)	38.21 (29.31)	33.32 (19.80)	0.587
24-h urinary protein (mg/24 h)	4.94 (1.42)	7.12 (4.68)	1.69 (1.13)	0.054
MAP (mmHg)	104.50 (10.04)	99.38 (10.48)	96.58 (9.20)	0.319

Data were expressed as mean (SD). Group 1: control group; group 2: diabetic group; group 3: diabetic + canagliflozin + losartan group. N, number of rats were observed in each group; BUN, blood urea nitrogen; Scr, serum creatinine; Ucr, urine creatinine; NAG, N-acetyl-glucosaminidase; MAP, mean arterial pressure.

and blood glucose levels of diabetic rats in group 3 returned to the normal range. Body weight, kidney-to-body weight ratio, BUN, Scr, NAG, 24-h urinary protein, and MAP did not differ significantly among the three groups (all P>0.05).

The elasticity values of the mid-portion of the renal cortex in the three groups are displayed in *Table 2*. The mean elasticity of the diabetic kidneys in group 2 was significantly higher than that of the normal kidneys in group 1 (P<0.01). Following 6 weeks of daily administration, the renal stiffness of the diabetic rats in group 3 significantly decreased, approaching levels similar to those of the normal group.

The cortical TICs rose steeply, quickly reaching peak intensity, and then slowly declined to the basal level. Compared with group 1, diabetic rats in group 2 exhibited higher and delayed enhancement, and they reached the signal intensity peaks more slowly and took longer time to develop into the wash-out phase, thus the areas under the ascending curve and the descending curve were larger (*Figure 4*).

Table 2 compiles the CEUS-derived values assessing signal intensity and time. The parameters peak enhancement (PE), wash-in area under the curve (WiAUC), wash-out AUC (WoAUC), wash-in and wash-out AUC (WiWoAUC), wash-in perfusion index (WiPI), rise time (RT), and time to peak (TTP) of group 2 were significantly higher than those of group 1 (all P<0.01). After drug

treatment, perfusion abnormalities in diabetic rats were effectively suppressed, and all perfusion parameters were not significantly different from those in normal rats (*Figure 5*). Additionally, no significant changes were observed in the parameters mean transit time local (mTTl), fall time (FT), wash-in rate (WiR), and wash-out rate (WoR) among the three groups (all P>0.05).

Pearson and Spearman correlation analysis indicated that cortical stiffness measured by SWE was positively correlated with those significantly altered CEUS-derived parameters (*Table 3*). The cortical stiffness was strongly correlated with WiAUC [r=0.701; 95% confidence interval (CI): 0.519–0.862; P<0.001], WoAUC (r=0.647; 95% CI: 0.390–0.789; P<0.001), and WiWoAUC (r=0.655; 95% CI: 0.398–0.794; P<0.001), and moderately correlated with PE (r=0.539; 95% CI: 0.301–0.743; P=0.001), WiPI (r=0.555; 95% CI: 0.304–0.724; P<0.001), RT (r=0.425; 95% CI: 0.150–0.681; P=0.010), and TTP (r=0.439; 95% CI: 0.129–0.686; P=0.007) (*Figure 6*).

Pathological examination showed that diabetic rats in group 2 developed structural changes such as glomeruli hypertrophy. After 6 weeks of drug treatment, the diabetic rats in group 3 showed no obvious structural changes compared to the normal rats in group 1 (*Figure 7*). Typical histopathological changes associated with DKD, such as significantly thickened glomerular basement membrane and mesangial sclerosis, were not observed in all three groups.

Table 2 The cortical stiffness and CEUS-derived quantitative parameters in each group

Parameters	Group 1			Group 2			Group 3			P value
	Mean	SD	Median (IQR)	Mean	SD	Median (IQR)	Mean	SD	Median (IQR)	
Stiffness (kPa)	16.8	1.1	16.7 (16.3–17.6)	27.4	3.8	28.0 (25.9–29.7)	19.9	1.6	20.1 (18.6–20.9)	<0.001
PE (a.u)	11,189.7	3,779.6	10,725.2 (8,122.3–12,317.0)	20,924.9	4,559.9	20,442.8 (18,225.5–23,246.9)	14,374.1	5,390.0	12,316.0 (9,818.2–19,009.8)	<0.001
WiAUC (a.u)	18,569.9	6,716.6	18,393.3 (12,108.2–24,450.4)	46,922.4	11,239.5	43,525.4 (40,692.6–59,750.6)	20,762.2	3,170.5	20,665.4 (17,581.4–24,040.5)	<0.001
RT (s)	2.7	0.9	2.4 (1.8–3.7)	3.6	0.9	3.4 (2.8–4.3)	2.4	0.6	2.5 (1.8–3.0)	0.003
mTTl (s)	27.4	13.3	22.3 (18.0–38.9)	29.3	9.2	25.6 (23.2–37.2)	28.4	9.5	26.3 (19.8–38.1)	0.916
TTP (s)	3.9	0.9	3.3 (3.2–4.9)	5.3	1.4	5.2 (4.3–6.8)	3.4	0.4	3.3 (3.0–3.9)	0.001
WiR (a.u)	7,038.7	3,521.5	5,380.2 (4,496.0–8,555.2)	9,473.8	3,753.2	9,653.9 (5,545.2–11,455.2)	9,936.2	5,613.4	7,594.3 (5,788.3–13,867.2)	0.155
WiPI (a.u)	7,183.9	2,317.0	6,731.3 (5,306.9–7,831.1)	13,486.8	2,931.3	13,152.7 (11,749.9–14,995.7)	9,242.9	3,255.5	8,160.0 (6,607.6–11,999.4)	<0.001
WoAUC (a.u)	45,159.0	22,051.7	40,481.9 (22,223.3–66,685.4)	105,180.9	43,524.1	96,104.1 (77,007.6–113,211.9)	46,121.1	9,066.7	42,059.7 (40,262.4–52,467.0)	<0.001
WiWoAUC (a.u)	63,728.9	27,762.1	57,467.9 (34,538.8–92,663.4)	152,103.3	52,614.3	143,591.3 (118,623.6–160,690.8)	66,883.3	10,749.4	64,708.5 (58,005.6–74,332.1)	<0.001
FT (s)	6.9	4.5	6.2 (3.1–8.5)	8.1	3.3	7.3 (5.8–8.8)	5.7	2.4	5.7 (3.6–7.0)	0.159
WoR (a.u)	2,640.0	1,884.4	1,812.6 (1,335.0–4,047.9)	3,320.7	1,574.9	3,052.4 (2,050.3–4,696.3)	3,777.8	3,195.0	2,352.5 (1,466.1–5,888.1)	0.370

Group 1: control group; group 2: diabetic group; group 3: diabetic + canagliflozin + losartan group. CEUS, contrast-enhanced ultrasound; SD, standard deviation; IQR, interquartile range; PE, peak enhancement; a.u, arbitrary unit; WiAUC, wash-in area under the curve; RT, rise time; mTTl, mean transit time local; TTP, time to peak; WiR, wash-in rate; WiPI, wash-in perfusion index; WoAUC, wash-out area under the curve; WiWoAUC, wash-in and wash-out area under the curve; FT, fall time; WoR, wash-out rate.

Discussion

Although CEUS and SWE have been widely applied in various clinical specialties, the stiffness and CEUS perfusion parameters of the kidney in the early stage of DM have not been sufficiently explored. Meanwhile, few studies have investigated the relationship between renal stiffness and perfusion. In the present study, CEUS and SWE techniques were employed to assess dynamic alterations in renal perfusion and cortical stiffness in a rat model of early DM. CEUS revealed increased renal blood flow and prolonged perfusion time, and SWE showed higher cortical stiffness in early diabetic rats. CEUS and SWE were able to show hemodynamic amelioration in diabetic rats treated with canagliflozin and losartan. Moreover, we revealed a significant positive correlation between stiffness and partial sensitive CEUS parameters.

STZ is a natural compound used to induce DM by selectively disrupting the function of islet β cells of animals. In the present study, the diabetic rats exhibited larger kidneys and higher blood glucose after intraperitoneal injection of STZ. The growth of the diabetic kidney primarily stems from the enlargement of nephrons, specifically the hypertrophy of proximal tubules (23). Besides, increased glomerular blood volume and flow velocity contribute to kidney weight (24). The absence of albuminuria, renal insufficiency, and other significant DKD phenotypes, along with the lack of typical pathological changes, strongly suggests that the diabetic rats included in the study were in the early stages of DKD.

The onset and progression of DKD is closely related to disturbances in renal hemodynamics, such as glomerular hypertension and/or hyperperfusion (24). The kidney is highly vascularized, more than 90% of the total renal
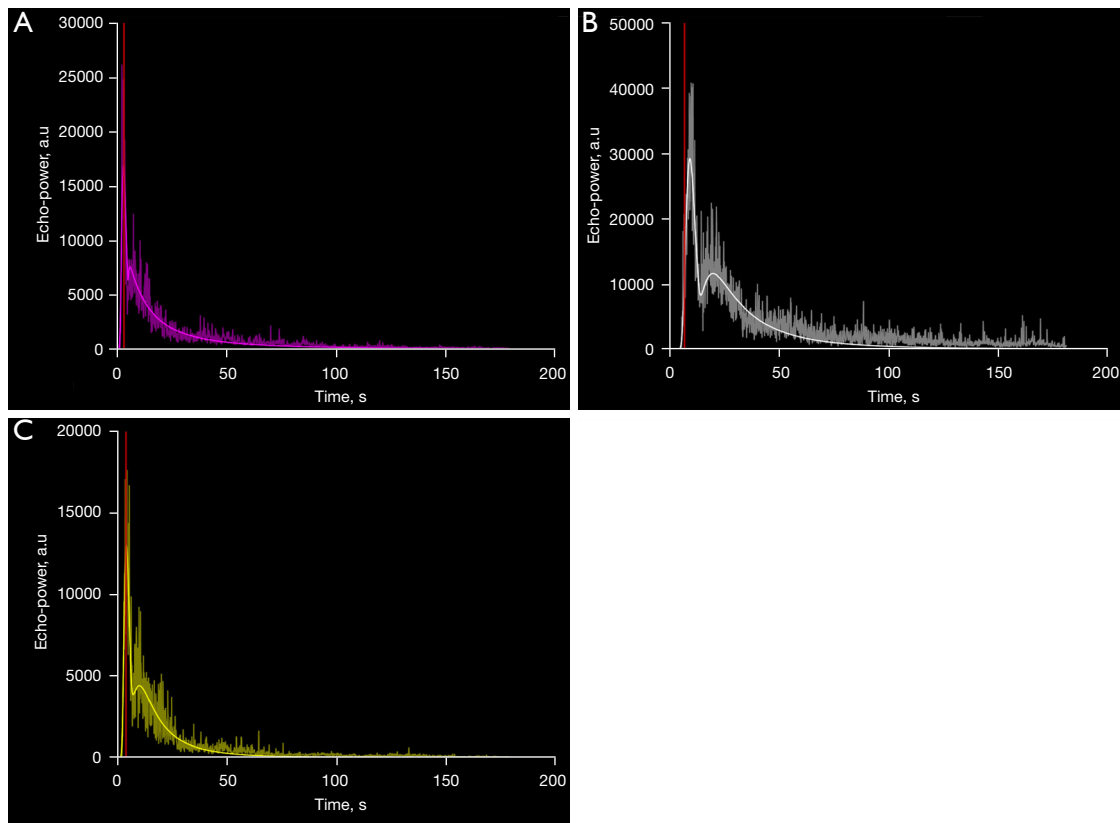
7674

Li et al. CEUS and SWE assess renal hemodynamics in early diabetes

Figure 4 Representative images showing the TICs of the three groups. (A) TIC for a normal rat in group 1, and RT was 1.6 s, TTP was 2.9 s, and mTTl was 32.7 s. (B) TIC for a diabetic rat in group 2, and RT was 3.5 s, TTP was 7.2 s, and mTTl was 26.4 s. (C) TIC for a diabetic rat after drug treatment in group 3, RT was 2.0 s, TTP was 4.1 s, and mTTl was 15.1 s. Group 1: control group; group 2: diabetic group; group 3: diabetic + canagliflozin + losartan group. a.u, arbitrary unit; TIC, time-intensity curve; RT, rise time; TTP, time to peak; mTTl, mean transit time local.

blood flow enters the renal cortex, so the cortex might be predominantly affected when the renal perfusion changes. CEUS is considered an ideal tool for real-time detection of renal parenchymal perfusion due to its safety, good tolerance, and reproducibility without renal toxicity. A number of previous studies have confirmed that CEUS can effectively evaluate renal hemodynamic abnormalities in DKD (25,26), but little is known about perfusion parameters in early diabetes with normal renal function, especially before the occurrence of irreversible pathological changes.

In our study, CEUS exhibited increased and delayed cortical enhancement in early-stage diabetic rats; blood volume-related parameters PE, WiAUC, WoAUC, and WiWoAUC were greater than they were in the control group. Previous studies on DKD have indicated that vasoactive factors exert a more significant influence on the afferent arterioles compared to the efferent arterioles,

and this discrepancy leads to a predominant dilation of the afferent artery (23,24). As a consequence, there is an increase in glomerular perfusion volume and glomerular hypertension in diabetic kidneys, which directly contributes to increased maximum contrast agent signal intensity (PE) and renal perfusion volume (WiAUC) in CEUS. WoAUC represents the clearance of renal perfusion, and an increased WoAUC suggests decreased clearance, which also contributes to the enhancement of renal perfusion. WiWoAUC represents the total change of renal perfusion and is influenced by both WiAUC and WoAUC. Additionally, the time-derived parameters RT and TTP, and the ratio between WiAUC and RT, known as WiPI, increased in the early stage of diabetes, indicating a prolongation of cortical perfusion time and an increase in average blood velocity within the renal cortex. These findings suggested that. PE, WiAUC, WoAUC, WiWoAUC, RT, TTP, and WiPI would be
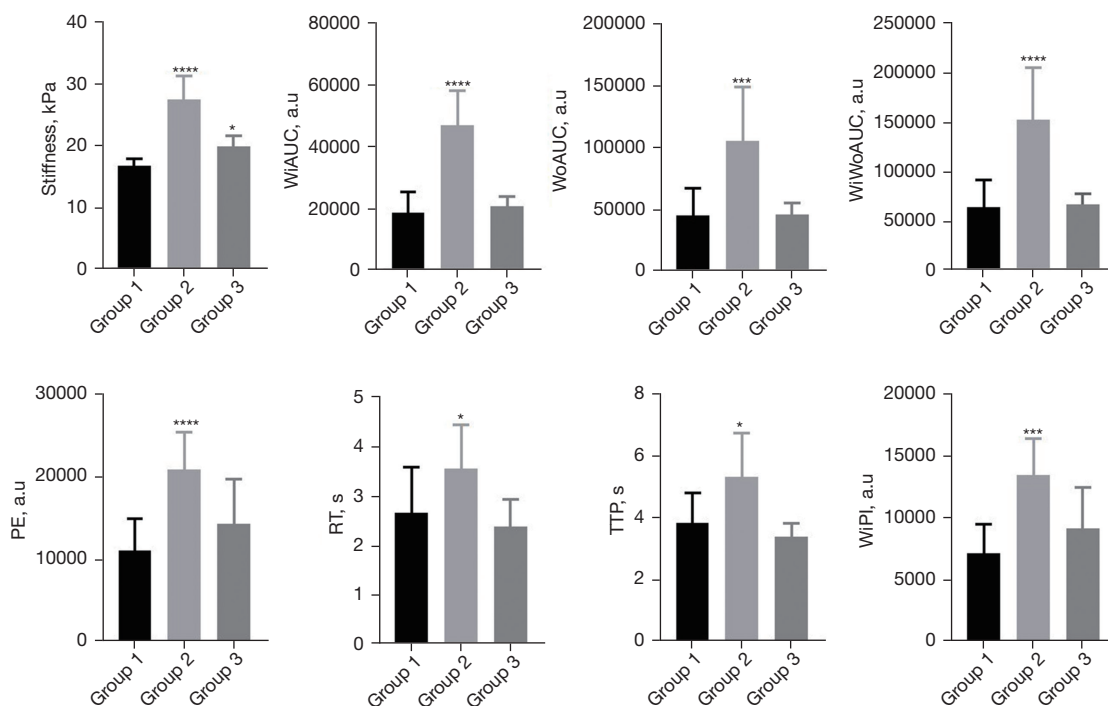
Figure 5 The histograms show the variation of cortical stiffness by SWE and partial CEUS-derived parameters in the three groups. Group 1: control group; group 2: diabetic group; group 3: diabetic + canagliflozin + losartan group. *, P<0.05; ***, P<0.001; ****, P<0.0001; n=6. WiAUC, wash-in area under the curve; a.u, arbitrary unit; WoAUC, wash-out area under the curve; WiWoAUC, wash-in and wash-out area under the curve; PE, peak enhancement; RT, rise time; TTP, time to peak; WiPI, wash-in perfusion index; SWE, shear wave elastography; CEUS, contrast-enhanced ultrasound.

Table 3 Correlation coefficient between cortical stiffness and CEUS quantitative parameters

Parameters	r (95% CI)	P value
PE (a.u)	0.539 (0.301–0.743)	0.001
WiAUC (a.u)	0.701 (0.519–0.862)	<0.001
RT (s)	0.425 (0.150–0.681)	0.010
TTP (s)	0.439 (0.129–0.686)	0.007
WiPI (a.u)	0.555 (0.304–0.724)	<0.001
WoAUC (a.u)	0.647 (0.390–0.789)	<0.001
WiWoAUC (a.u)	0.655 (0.398–0.794)	<0.001

CEUS, contrast-enhanced ultrasound; CI, confidence interval; PE, peak enhancement; a.u, arbitrary unit; WiAUC, wash-in area under the curve; RT, rise time; TTP, time to peak; WiPI, wash-in perfusion index; WoAUC, wash-out area under the curve; WiWoAUC, wash-in and wash-out area under the curve.

valuable parameters for CEUS to assess renal perfusion in early diabetes.

SWE is a reproducible, non-invasive method for evaluating kidney stiffness. Quantifying renal stiffness is complex because its results are not only related to fibrosis, as it also sensitive to mechanical and functional parameters such as anisotropy, vascularization, and external pressure (27). In this study, we applied minimal scanning pressure to measure elasticity in the mid-portion of the renal cortex, the measurement location recommended by previous scholars (28,29). This approach aimed to minimize the variations caused by higher structural anisotropy and external pressure, and to improve the validity and reliability of the elasticity measurements. In this study, the mean stiffness of diabetic kidneys was 27.39 kPa, which was significantly higher than that of normal kidneys (16.76 kPa).
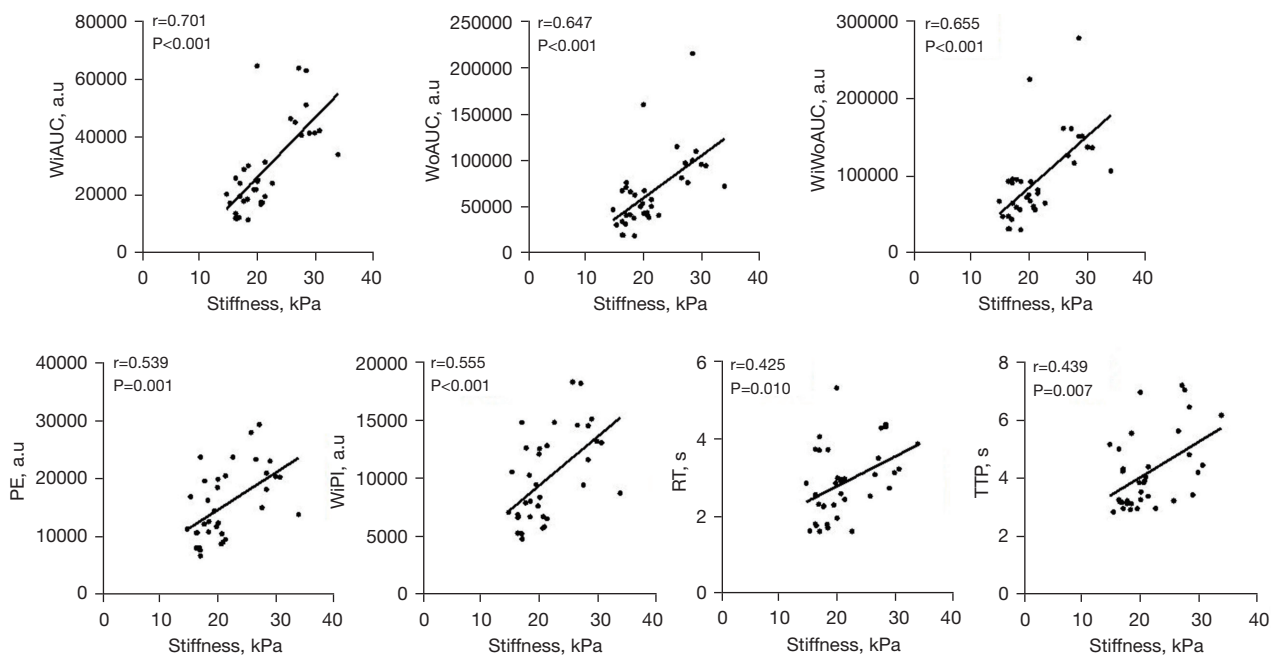
Figure 6 The relationships between cortical stiffness by SWE and CEUS-derived parameters that differed significantly among the three groups. WiAUC, wash-in area under the curve; a.u, arbitrary unit; WoAUC, wash-out area under the curve; WiWoAUC, wash-in and wash-out area under the curve; PE, peak enhancement; WiPI, wash-in perfusion index; RT, rise time; TTP, time to peak; SWE, shear wave elastography; CEUS, contrast-enhanced ultrasound.

The pathological examination revealed no obvious glomerular sclerosis and interstitial fibrosis, so the increase in cortical elasticity was mainly due to increased blood volume and glomerular hypertension, consistent with previous research which indicated the cortical elasticity was more prone to renal perfusion (30).

To further elucidate the role of CEUS and SWE in monitoring renal hemodynamics, the diabetic rats were treated with the selective angiotensin II receptor blocker (ARB) losartan and the sodium-glucose cotransporter 2 (SGLT2) inhibitor canagliflozin. SGLT2 inhibitors have emerged as an effective antihyperglycemic treatment and are recommended as part of glycemic management (31). There is increasing evidence that ARB can improve glomerular hemodynamics due to greater suppression in efferent than in afferent arteriolar resistance (32). After 6 weeks of daily administration, renal stiffness in the treated rats decreased significantly, approaching levels similar to the normal group. Besides, the altered perfusion parameters also recovered, and there were no significant differences in CEUS parameters between the treated rats and the normal rats. Furthermore, pathological examination revealed that the structural changes observed in the diabetic kidneys were improved after drug treatment. These findings indicated that early intervention with strict drug treatment is able to ameliorate renal pathologic changes in early diabetes by normalization of renal hemodynamics.

Furthermore, we analyzed the correlation between kidney elasticity measured by SWE and the CEUS quantitative parameters. The results revealed that stiffness was strongly positively correlated with perfusion volume parameters AUC (WiAUC, WoAUC, and WiWoAUC), especially WiAUC (r=0.701, P<0.001), and moderately positively correlated with PE, WiPI, RT, and TTP. Taken together, these results indicated that renal hemodynamics in early diabetic rats were characterized by increased cortical stiffness and both delayed and increased cortical perfusion. CEUS and SWE can sensitively detect renal hemodynamics during the early stages of the disease and facilitate timely treatment.

This study has several limitations. First, CEUS and SWE are usually local evaluations of a single section, and the results are operator-dependent. Considering the complexity of the renal structure, it is necessary to establish standardized procedure (33). In this study, we performed CEUS and SWE detection of the kidney at a specific
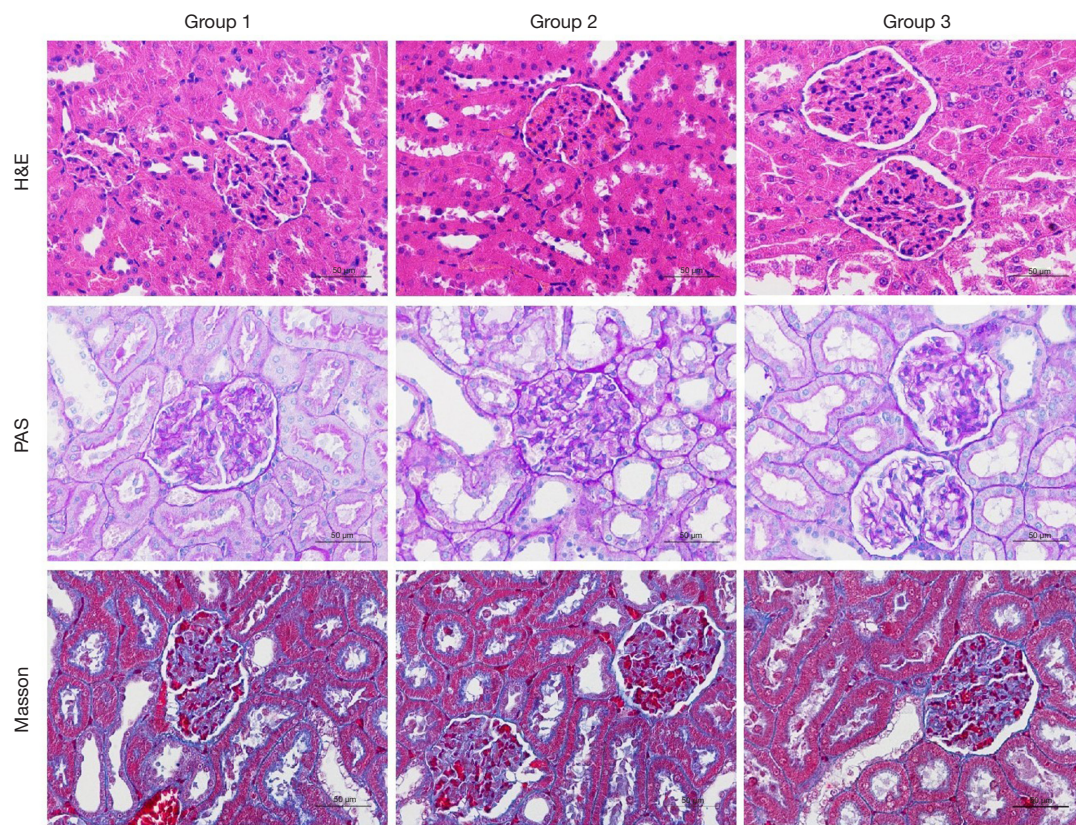
Figure 7 Histological morphology of the kidneys in three groups. H&E, PAS, and Masson staining of kidney sections were compared between different groups of rats. Glomeruli hypertrophy was observed in group 2. No typical histopathologic changes associated with diabetes were observed in the three groups (n=6). Group 1: control group; group 2: diabetic group; group 3: diabetic + canagliflozin + losartan group. Scale bars: 50 μm. H&E, hematoxylin and eosin; PAS, periodic acid-Schiff.

location along the largest longitudinal section to obtain reliable and reproducible results. This was a preliminary study using SWE to assess renal hemodynamics in early diabetic rats, and its effectiveness could be further validated with other well-established models. Third, no universal agreement on the use of certain CEUS quantitation parameters in DM has been reached, and the normal range on CEUS parameters and stiffness needs to be further studied.

Conclusions

CEUS is a promising tool for early detection of hemodynamic abnormalities in the early phase of diabetes without specific histopathological changes in the kidney. Besides, cortical stiffness measured by SWE positively correlates with some CEUS quantitative parameters and can be a potential tool for predicting renal hemodynamics

in early diabetes. However, further evidence is required before clinical practice.

Acknowledgments

Footnote

Reporting Checklist: The authors have completed the ARRIVE reporting checklist. Available at https://qims.amegroups.com/article/view/10.21037/qims-23-409/rc

Conflicts of Interest: All authors have completed the ICMJE

uniform disclosure form (available at https://qims.amegroups.com/article/view/10.21037/qims-23-409/coif). The authors have no conflicts of interest to declare.

Ethical Statement: The authors are accountable for all aspects of the work in ensuring that questions related to the accuracy or integrity of any part of the work are appropriately investigated and resolved. The study was approved by the Biomedical Ethics Committee of Peking University (No. LA2021585), in compliance with international AAALAC guidelines for the care and use of animals.

Open Access Statement: This is an Open Access article distributed in accordance with the Creative Commons Attribution-NonCommercial-NoDerivs 4.0 International License (CC BY-NC-ND 4.0), which permits the non-commercial replication and distribution of the article with the strict proviso that no changes or edits are made and the original work is properly cited (including links to both the formal publication through the relevant DOI and the license). See: https://creativecommons.org/licenses/by-nc-nd/4.0/.

References

1. Selby NM, Taal MW. An updated overview of diabetic nephropathy: Diagnosis, prognosis, treatment goals and latest guidelines. Diabetes Obes Metab 2020;22 Suppl 1:3-15.
2. Oshima M, Shimizu M, Yamanouchi M, Toyama T, Hara A, Furuichi K, Wada T. Trajectories of kidney function in diabetes: a clinicopathological update. Nat Rev Nephrol 2021;17:740-50.
3. Comai G, Malvi D, Angeletti A, Vasuri F, Valente S, Ambrosi F, Capelli I, Ravaioli M, Pasquinelli G, D'Errico A, Fornoni A, La Manna G. Histological Evidence of Diabetic Kidney Disease Precede Clinical Diagnosis. Am J Nephrol 2019;50:29-36.
4. Mustafa S, Elgazzar AH, Kamal N. Effect of Verapamil on Kidney Function Using Radionuclide Imaging. Pharmacology 2019;103:173-8.
5. Jiang K, Ferguson CM, Abumoawad A, Saad A, Textor SC, Lerman LO. A modified two-compartment model for measurement of renal function using dynamic contrast-enhanced computed tomography. PLoS One 2019;14:e0219605.
6. Rudnick MR, Leonberg-Yoo AK, Litt HI, Cohen RM, Hilton S, Reese PP. The Controversy of Contrast-Induced Nephropathy With Intravenous Contrast: What Is the Risk? Am J Kidney Dis 2020;75:105-13.
7. Lim SW, Chrysochou C, Buckley DL, Kalra PA, Sourbron SP. Prediction and assessment of responses to renal artery revascularization with dynamic contrast-enhanced magnetic resonance imaging: a pilot study. Am J Physiol Renal Physiol 2013;305:F672-8.
8. Zhang JL, Lee VS. Renal perfusion imaging by MRI. J Magn Reson Imaging 2020;52:369-79.
9. Wang L, Mohan C. Contrast-enhanced ultrasound: A promising method for renal microvascular perfusion evaluation. J Transl Int Med 2016;4:104-8.
10. McArthur C, Baxter GM. Current and potential renal applications of contrast-enhanced ultrasound. Clin Radiol 2012;67:909-22.
11. Wang Y, Zhao P, Li N, Dong Z, Lin L, Liu J, Liang S, Wang Q, Tang J, Luo Y. A Study on Correlation between Contrast-Enhanced Ultrasound Parameters and Pathological Features of Diabetic Nephropathy. Ultrasound Med Biol 2022;48:228-36.
12. Zhao P, Li Q, Wang S, Wang Y, Zhu J, Zhu L, Tang J, Luo Y. Quantitative Analysis of Renal Perfusion in Rhabdomyolysis-Induced Acute Kidney Injury Using Contrast-Enhanced Ultrasound: An Experimental Study. Ultrasound Med Biol 2022;48:2110-8.
13. He L, Li Z, Zhang Q, Chen Y, Gao Y, Chen T, Wang N, Jiang L, Fan Y. Evaluation of renal microperfusion in hyperuricemic nephropathy by contrast-enhanced ultrasound imaging. Dis Model Mech 2022;15:dmm049382.
14. Bob F, Grosu I, Sporea I, Bota S, Popescu A, Sima A, Șirli R, Petrica L, Timar R, Schiller A. Ultrasound-Based Shear Wave Elastography in the Assessment of Patients with Diabetic Kidney Disease. Ultrasound Med Biol 2017;43:2159-66.
15. Golatta M, Pfob A, Büsch C, Bruckner T, Alwafai Z, Balleyguier C, Clevert DA, Duda V, Goncalo M, Gruber I, Hahn M, Kapetas P, Ohlinger R, Rutten M, Tozaki M, Wojcinski S, Rauch G, Heil J, Barr RG. The Potential of Shear Wave Elastography to Reduce Unnecessary Biopsies in Breast Cancer Diagnosis: An International, Diagnostic, Multicenter Trial. Ultraschall Med 2023;44:162-8.
16. Chen S, Sanchez W, Callstrom MR, Gorman B, Lewis JT, Sanderson SO, Greenleaf JF, Xie H, Shi Y, Pashley M, Shamdasani V, Lachman M, Metz S. Assessment of liver viscoelasticity by using shear waves induced by ultrasound radiation force. Radiology 2013;266:964-70.
17. Derieppe M, Delmas Y, Gennisson JL, Deminière C, Placier S, Tanter M, Combe C, Grenier N. Detection of

intrarenal microstructural changes with supersonic shear wave elastography in rats. Eur Radiol 2012;22:243-50.

18. Yoon H, Lee YS, Lim BJ, Han K, Shin HJ, Kim MJ, Lee MJ. Renal elasticity and perfusion changes associated with fibrosis on ultrasonography in a rabbit model of obstructive uropathy. Eur Radiol 2020;30:1986-96.

19. Grenier N, Poulain S, Lepreux S, Gennisson JL, Dallaudière B, Lebras Y, Bavu E, Servais A, Meas-Yedid V, Piccoli M, Bachelet T, Tanter M, Merville P, Couzi L. Quantitative elastography of renal transplants using supersonic shear imaging: a pilot study. Eur Radiol 2012;22:2138-46.

20. Asano K, Ogata A, Tanaka K, Ide Y, Sankoda A, Kawakita C, Nishikawa M, Ohmori K, Kinomura M, Shimada N, Fukushima M. Acoustic radiation force impulse elastography of the kidneys: is shear wave velocity affected by tissue fibrosis or renal blood flow? J Ultrasound Med 2014;33:793-801.

21. Wang L, Xia P, Lv K, Han J, Dai Q, Li XM, Chen LM, Jiang YX. Assessment of renal tissue elasticity by acoustic radiation force impulse quantification with histopathological correlation: preliminary experience in chronic kidney disease. Eur Radiol 2014;24:1694-9.

22. Wang G, Zhang X, Lu X, Liu J, Zhang Z, Wei Z, Wu Z, Wang J. Fish oil supplementation attenuates cognitive impairment by inhibiting neuroinflammation in STZ-induced diabetic rats. Aging (Albany NY) 2020;12:15281-9.

23. Vallon V, Komers R. Pathophysiology of the diabetic kidney. Compr Physiol 2011;1:1175-232.

24. Li B, Yao J, Kawamura K, Oyanagi-Tanaka Y, Hoshiyama M, Morioka T, Gejyo F, Uchiyama M, Oite T. Real-time observation of glomerular hemodynamic changes in diabetic rats: effects of insulin and ARB. Kidney Int 2004;66:1939-48.

25. Wang L, Wu J, Cheng JF, Liu XY, Ma F, Guo LH, Xu JM, Wu T, Mohan C, Peng A, Xu HX, Song YX. Diagnostic value of quantitative contrast-enhanced ultrasound (CEUS) for early detection of renal hyperperfusion in diabetic

kidney disease. J Nephrol 2015;28:669-78.

26. Ma F, Cang Y, Zhao B, Liu Y, Wang C, Liu B, Wu T, Song Y, Peng A. Contrast-enhanced ultrasound with SonoVue could accurately assess the renal microvascular perfusion in diabetic kidney damage. Nephrol Dial Transplant 2012;27:2891-8.

27. Grenier N, Gennisson JL, Cornelis F, Le Bras Y, Couzi L. Renal ultrasound elastography. Diagn Interv Imaging 2013;94:545-50.

28. Bob F, Bota S, Sporea I, Sirli R, Petrica L, Schiller A. Kidney shear wave speed values in subjects with and without renal pathology and inter-operator reproducibility of acoustic radiation force impulse elastography (ARFI)--preliminary results. PLoS One 2014;9:e113761.

29. Leong SS, Wong JHD, Md Shah MN, Vijayananthan A, Jalalonmuhali M, Mohd Sharif NH, Abas NK, Ng KH. Stiffness and Anisotropy Effect on Shear Wave Elastography: A Phantom and in Vivo Renal Study. Ultrasound Med Biol 2020;46:34-45.

30. Liu X, Li N, Xu T, Sun F, Li R, Gao Q, Chen L, Wen C. Effect of renal perfusion and structural heterogeneity on shear wave elastography of the kidney: an in vivo and ex vivo study. BMC Nephrol 2017;18:265.

31. Davies MJ, D'Alessio DA, Fradkin J, Kernan WN, Mathieu C, Mingrone G, Rossing P, Tsapas A, Wexler DJ, Buse JB. Management of Hyperglycemia in Type 2 Diabetes, 2018. A Consensus Report by the American Diabetes Association (ADA) and the European Association for the Study of Diabetes (EASD). Diabetes Care 2018;41:2669-701.

32. Arima S, Ito S. The mechanisms underlying altered vascular resistance of glomerular afferent and efferent arterioles in diabetic nephropathy. Nephrol Dial Transplant 2003;18:1966-9.

33. Lin L, Wang Y, Yan L, Li N, Tian X, Li Q, Tang J, Luo Y. Interobserver reproducibility of contrast-enhanced ultrasound in diabetic nephropathy. Br J Radiol 2022;95:20210189.